JOURNAL OF Applied Polymer SCIENCE

Preparation and Electrochemical Properties of Poly-2,5-dihydroxyaniline/Activated Carbon Composite Electrode in Organic Electrolyte

Miao Sun, Wei Wang, Benlin He, Mingliang Sun, Wei Liu, Honglun Ge, Qinjie Zhang, Fan Sun
Institute of Material Science and Engineering, Ocean University of China, Qingdao 266100, Shandong Province, People's Republic of China
Correspondence to: W. Wang (E-mail: clwang@ouc.edu.cn) or B. He (E-mail: blhe@ouc.edu.cn)

ABSTRACT: Poly-2,5-dimethoxyaniline coating has been fabricated on active carbon (AC) substrates by cyclic voltammetry (CV) in organic system. The resulted coating is hydrolyzed to produce poly-2,5-dihydroxyaniline (PDHA) to enhance the capacitance of the composite electrode. Scanning electron microscope, Fourier transform infrared spectroscopy, X-ray diffraction, Raman spectra, CV, electrochemical impedance spectroscopy, and galvanostatic charge/discharge test are used to investigate the properties of these electrodes. In organic electrolyte, due to the introduced hydroquinone units, high value of capacitance up to 975 F g^{-1} of the PDHA/AC has been obtained at a current density of 0.37 A g^{-1} at a potential window of 0–1.5 V. An asymmetric capacitor has been assembled with the PDHA/AC positive and pure AC negative electrodes, which is able to obtain a specific energy as high as 178 Whkg^{-1} in the potential range of 0–2.0 V at a current density of 0.93 A g^{-1}. © 2012 Wiley Periodicals, Inc. J. Appl. Polym. Sci. 000: 000–000, 2012

KEYWORDS: poly-2,5-dihydroxyaniline; poly-2,5-dimethoxyaniline; organic electrolyte; hydroquinone; capacitance; supercapacitor

Received 11 January 2012; accepted 19 May 2012; published online
DOI: 10.1002/app.38069

INTRODUCTION

Conducting polymers are generally attractive as they have high charge density, low cost (compared with the relatively expensive metal oxides), outstanding properties, and numerous possible applications.[1,2] Conjugated polymers have an alternating single and double bonds between the atoms, especially carbon atoms, sometimes carbon–nitrogen atoms[3] and be used for electrically conducting materials such as electrode materials.

In recent years, composite electrode materials have been investigated by many researchers.[4–6] It is well known that conjugated polymers such as polyaniline (PANI),[7] polypyrrole,[8] and polythiophene[9] can improve the electrochemical performance of carbon based supercapacitors, as they can contribute pseudocapacitance to the total capacitance apart from the double-layer capacitance of carbon materials. Conjugated polymers typically have good conductivity in their doped state, they also display fast, reversible, and stable electrochemical behavior.[10] Polyaniline is one of the most important conducting polymers because of its economic viability, easy processability, high conductivity, and good environmental stability.[11,12] Large variety of applications of PANI such as electrochromic devices,[13] secondary batteries,[14] microwave absorber in electromagnetic shielding[15] and catalysis[16] were studied by many researchers. The disubstituted derivatives of PANI are also potential candidates in many technological applications. Preparation and electrochemical properties of PANI/active carbon (AC) composite electrode have been a subject of several studies.[17–19] However, hardly any attempt has been made to investigate the electrode of poly-2,5-dihydroxyaniline (PDHA) coating on AC substrates. DMA is a disubstituted derivative of aniline with methoxy (—OCH_3) groups substituted at *ortho*- and *meta*-positions.[20] With the existence of two methoxy groups on each aniline ring within aniline, the potential required for its electropolymerization is lowered greatly compared with aniline.[21] Poly-2,5-dimethoxyaniline (PDMA) can be easily oxidized from leucoemeraldine (LE) to emeraldine (E) state in comparison of PANI.[22] The presence of two electron donor substituents induces some interesting properties of the resulting polymer.[23]After the methoxy groups (—OCH_3) hydrolyzed into hydroxyl groups (—OH) to produced PDHA, the interaction of introduced hydroquinone units and quinone in the PDHA polymer enhanced the conductivity of the electrode. The structural transformation is as follow:

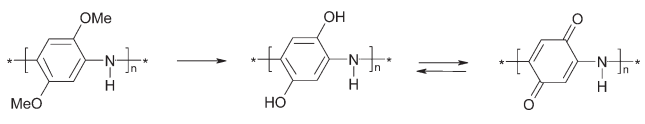

PDMA can be hydrolyzed to PDHA in natural environment in the influence of water very slowly, in this study, we use cyclic voltammetry (CV) to show the hydrolysis process of PDMA to produce PDHA with the methoxy groups (—OCH_3) hydrolyzed into hydroxyl groups (—OH). Our team has studied PDHA/AC composite electrode in 0.5*M* H_2SO_4 aqueous system only with a charge/discharge potential window of 0–0.8 V.[24] In that case, the PDHA/AC composite electrode usually shows a lower energy density (ED) according to the equation[25]:

$$\mathrm{ED} = \frac{1}{2}\mathrm{CV}^2 \quad (1)$$

where *C* and *V* are the capacitance and operating voltage of the supercapacitor, respectively. Based on eq. (1), two methods can be considered to enhance the ED of a supercapacitor. One is to increase the specific capacitance of the electrode material and the other is to increase the operating voltage. Because the ED of a supercapacitor is proportional to the square of the operating voltage, the latter method is a more effective way to improve the ED. Composite electrodes test in aqueous electrolytes may get a low specific energy (Wh kg^{-1}), because of their restricted potential window of about 1 V.[26–29] So, the development of composite electrodes using organic electrolytes is quite important in enhancing the energy and power density of the supercapacitors.

In this work, due to the existence of introduced hydroquinone units, high value of capacitance up to 975 F g^{-1} of the PDHA/AC had been obtained at a current density of 0.37 A^{-1}, which was much higher than that of PDMA/AC composite electrode (751 F g^{-1}) at a potential window from 0 to 1.5 V. The electrochemical properties of PDHA/AC electrode in organic electrolyte have been studied in detail. Although the obtained specific capacitance of PDHA /AC composite electrode was close to that in aqueous electrolyte, we utilize organic electrolyte to assemble PDHA /AC composite electrode as positive electrode and AC electrode as negative electrode in supercapacitor to obtain the ED as high as 178 Whkg^{-1} at a current density of 0.93 A g^{-1} by increasing the charge/discharge potential window from 0 to 2.0 V.

EXPERIMENTAL

Materials

2,5-Dimethoxyaniline (DMA), activated carbon powders (specific surface area: >2000 m^2 g^{-1}), carbon black, polyvinylidene fluoride (PVDF), lithium perchlorate ($LiClO_4$), distilled acetonitrile (ACN), acetic acid, *N*-methyl pyrrolidone (NMP), acetone, sulfuric acid (H_2SO_4) were purchased Sinopharm Co. and used as received. Deionized water was employed to prepare all solutions.

Preparation of AC Electrode

Porous activated carbon powders, PVDF, carbon black were mixed in the mass ratio of 8:1:1. Thirty milliliters of NMP was added to the above mixture to form the slurry by heating and stirring to evaporate the solvent NMP. Coating the slurry evenly on a stainless steel mesh which was degreased ultrasonically with acetone and rinsed with ethanol, and the geometric area of this stainless steel mesh substrate was 1 cm × 1 cm. The stainless steel mesh and the resultant AC electrode were weighed by electronic balance after being dried in a vacuum oven at 353 K for 4 h.

Preparation of PDHA/AC Composite Electrode

The stainless steel mesh was tested in acetonitrile solution containing 1*M* $LiClO_4$ by CV between −0.2 and 2.0 V. The PDMA coating was synthesized on activated carbon substrate by CV method in the acetonitrile solution containing 0.2*M* monomer, 1*M* $LiClO_4$ (used as the supporting electrolyte), 1*M* acetic acid. The potential for PDMA was cycled between −0.2 and 1.2 V. The obtained PDMA/AC electrode was hydrolyzed to produce PDHA/AC in 0.5*M* H_2SO_4 solution through CV in a potential range between −0.2 and 0.8 V. The hydrolysis of PDHA was carried out via nine CV cycles in a scanning rate of 1 mVs^{-1}. After being rinsed with twice distilled water, the electrode was dried in a vacuum oven at 323 K for 1 h and then weighed by electronic balance.

Measurements

All electrochemical experiments were performed by using a three electrode configuration, with AC or PDMA/AC, PDHA/AC as the working electrode (1 cm^2), platinum gauze electrode (1 cm^2) as counter electrode and Ag/AgCl electrode as reference electrode. The identical method was utilized to prepare PDMA and PDHA films on glass electrode for comparison of their structures without the infrared absorption of activated carbon. The Fourier transform infrared (FTIR) spectra of PDMA and PDHA were recorded in the spectral range 4000–400 cm^{-1} using a Bruker TENSOR 27 FTIR spectrometer. X-ray diffraction (XRD) measurements were performed on Bruker AXS D8 Advance. Raman spectra were taken at a green laser line (532 nm) over the 400–4000 cm^{-1} region using a Renishaw–Raman Spectrometer InVia from with microscope facility. The morphologies of samples were observed by the field-emission scanning electron microscopy (FE-SEM, JEOL-JSM-6700F). CV tests were carried out by using an electrochemical work station LK9805Z (Lanlike Company, Tianjin). The charge/discharge performance of these electrodes was examined by chronopotentiometry by using LAND CT2001A (Jinnuo Company, Wuhan). The Impedance Spectrum Analyzer, IM6 (ZAHNER, Germany), with Thales software was employed to measure the ac impedance spectra of electrodes at applied Potential of 1.0 V. The potential amplitude of ac was kept as 5 mV, and a wide frequency range of 10 mHz to 100 kHz was used. The mass of all active materials was weighed by BS 224S electronic balance (Sartorius Company Germany, $d = 0.1$ mg).

RESULTS AND DISCUSSION

Morphological Analysis

Figure 1 is a magnification by 10,000 and 20,000 times for the morphological properties of AC [Figure 1(a, b)] and PDHA/AC [Figure 1(c, d)] electrodes. The surface of the AC electrode is smooth and clean, and after deposited with PDHA, the surface of AC are uniformly covered by PDHA film which displays an interlinked porous network morphology, there are no apparent of AC in the PDHA film matrices which reveals that there are strong interactions between the polymer molecules and AC.

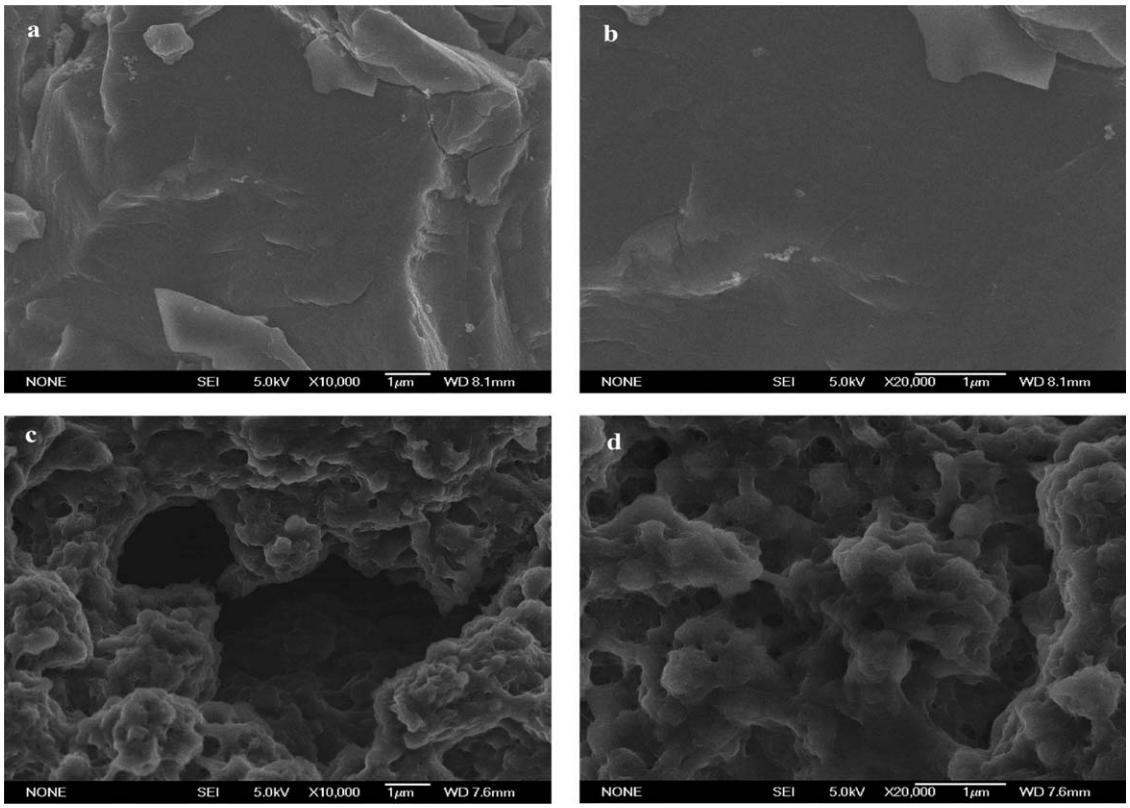

Figure 1. SEM photographs of AC (a, b) and PDHA/AC (c, d) electrodes.

Compared with AC electrode, the porous morphology may contribute more pathways through the network to make contact between the electrode materials and electrolyte ions more complete, leading to high charge storage and fast charge/discharge processes. The morphological properties reveal that the contact specific surface area between electrolyte ions and active material electrode is large, it is favorable to make the PDHA/AC electrode having more available active sites for faradic reaction which can lead to a higher specific capacitance compare with AC electrode.

XRD Analysis

Figure 2 shows powder X-ray diffraction patterns of PDHA/AC composite samples. The peaks of 22.5° and 28.5° are attributable to the AC substrate. The peaks appeared at 15°, 18.4°, and 24.9°, corresponding, respectively, to (0 1 1), (0 2 0), and (2 0 0) reflections of PDHA in its emeraldine salt form.[30] Because the certain steric hindrance caused by the existence of hydroxyl, PDHA presents a semicrystalline structure.

FTIR Spectroscopy of PDMA and PDHA Coatings

The identical method was utilized to prepare PDMA and PDHA films on glass electrode for comparison of their structures without the infrared absorption of activated carbon. The sample was dried in vacuum, deducted baseline in the test process (the air was the background for baseline, software automatically deduct). The FTIR spectrum of PDMA coating [Figure 3(a)] exhibits the following spectral features: (i) The strong peak at band $\sim$ 1520 cm^{-1} represents the stretching vibrations of the benzoid (B) rings and the shoulder peak at $\sim$ 1590 cm^{-1} is an indicative of stretching vibrations of quinoid (Q) rings,[31] this structure conversion is illustrated in Figure 4(a).

The FTIR spectrum of PDHA coating [Figure 3(b)] is a little different from those of [Figure 3(a)]. It shows the presence of phenolichydroxyl, the main bands corresponding to the C—H stretching vibrations by the influence of oxygen atom in the methoxy group at $\sim$ 2928 cm^{-1} and $\sim$ 2822 cm^{-1} are not observed, this reveal that the methoxy (—OCH_3) groups were hydrolyzed to hydroxyl groups (—OH).[32] Compared with

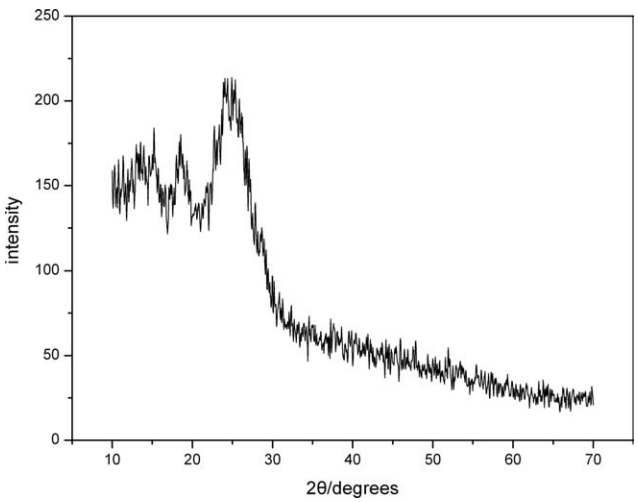

Figure 2. X-ray patterns of PDHA/AC composite samples.

Applied Polymer SCIENCE

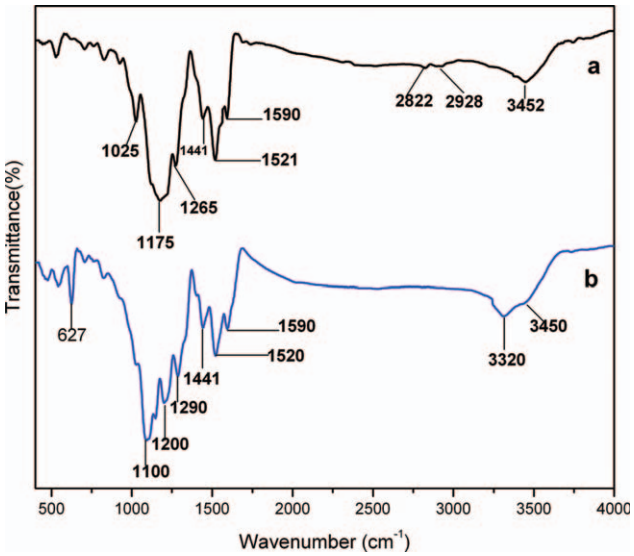

Figure 3. FTIR spectra of PDMA and PDHA: (a) PDMA and (b) PDHA. [Color figure can be viewed in the online issue, which is available at wileyonlinelibrary.com.]

[Figure 3(a)] this spectrum exhibits the following particular spectral features: (i) The band at ~ 3320 cm^{-1} shows the presence of hydroxyl groups (—OH). (ii) The band at ~ 1200 cm^{-1} is an indicative of carbonyl groups (C=O).[32] The result proves the presents of hydroquinone, and its structure conversion is shown in Figure 4(b). Similar to PDMA, (iii) the strong peak at band ~ 1520 cm^{-1} represents the stretching vibrations of the benzoid (B_h) rings in PDHA and the shoulder peak at ~ 1590 cm^{-1} is an indicative of stretching vibrations of the quinone (Q_h) rings in PDHA. The above structure conversion is shown in Figure 4(c).

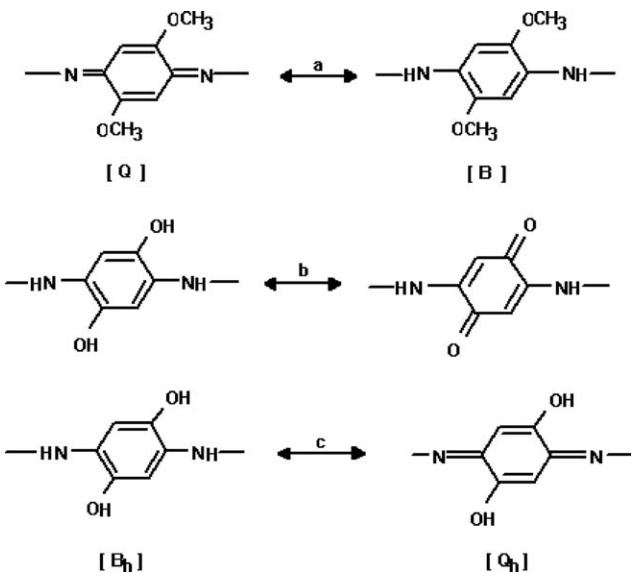

Figure 4. Molecular structure reflected by FTIR spectra: (a) quinoid (Q) rings and benzoid (B) rings in PDMA, (b) phenolichydroxyl and hydroquinone in PDHA, (c) benzoid (B_h) rings and quinone (Q_h) rings in PDHA.

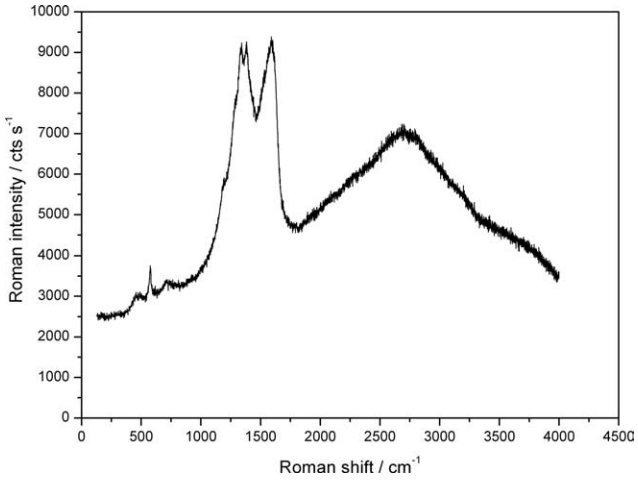

Figure 5. Raman spectra of PDHA/AC composite samples obtained with a green laser line $\lambda_o = 532$ nm.

Roman Spectroscopy Analysis

Raman spectra of PDHA/AC in Figure 5 is obtained with a green laser line $\lambda_o = 532$ nm. Sariciftci and Kuzmany[33] observed with the reduced form of PANI a strong band at 1624 cm^{-1} with green laser excitation (514.5 nm), and ascribed this band to a benzoid ring stretching vibration. Based on the literature[34] the band observed around 1600 cm^{-1} can be assigned to the benzoid mode. The band at 1332 cm^{-1} represents C—N stretching of semiquinone stretching and the band at 1386 cm^{-1} is an indicative of C=N stretching of quinone stretching. The peak at band 577 cm^{-1} represents C—H ring in-plane deformation; the band at 2700 cm^{-1} shows the presence of hydroxyl groups (—OH).

CV Test

CV Test of the Stainless Steel Mesh. In Figure 6, the stainless steel mesh is tested in acetonitrile solution containing 1*M* $LiClO_4$ by CV between −0.2 and 2.0 V. In the potential of −0.2 to 2.0 V, the stainless steel is not polarization, which proves that

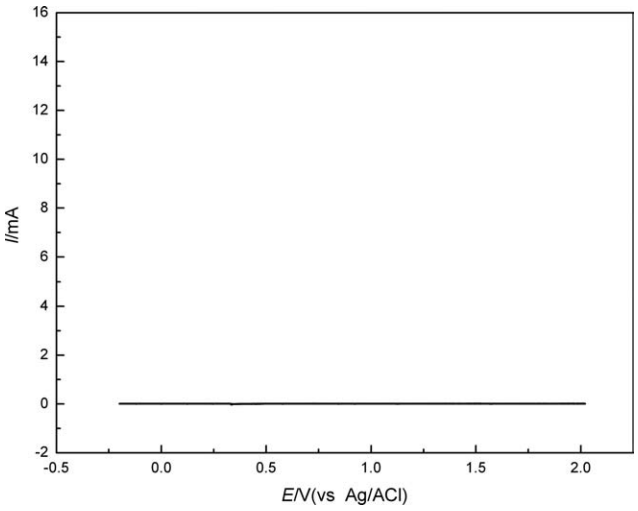

Figure 6. The CV test of stainless steel mesh in acetonitrile solution containing 1*M* $LiClO_4$ between −0.2 and 2.0 V.

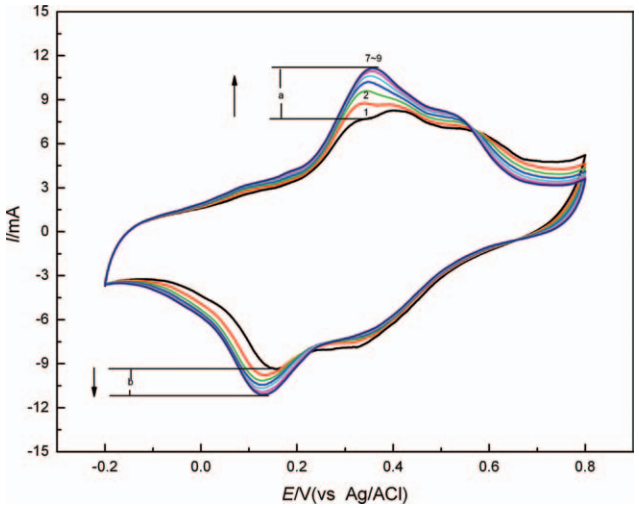

Figure 7. Cyclic voltammograms recorded of hydrolysis of PDMA/AC electrode in 0.5*M* H_2SO_4 for night (1–9) cycles. Potential range = −0.2 to 0.8 V (vs. Ag/AgCl); scan rate = 1 mVs^{-1}. [Color figure can be viewed in the online issue, which is available at wileyonlinelibrary.com.]

the stainless steel mesh is a suitable substrate material in the voltage study of −0.2 to 2.0 V.

CV Recorded of the Hydrolysis of PDMA/AC Composite Electrodes. In Figure 7, the first CV cycle reveals the properties of PDMA/AC. In the second cycle, the new peaks currents at 0.1 and 0.3 V display increasing in the successive cycles, which reveals the methoxy groups (—OCH_3) hydrolyzed into hydroxyl groups (—OH). Compared with the second cycle, the current of oxidation peak at 0.3 V and the current of reductive peak at 0.1 V increase as shown in Figure 7. This process is fully stabilized after seven cycles. The introduced hydroquinone units in the structure enhance the conductivity of the PDMA/AC electrode.[35] This conclusion is consistent with the structure transformation in Figure 4.

CV Measurement of AC, PDMA/AC, and PDHA/AC Electrodes. Figure 8(1) shows the CV record of AC, PDMA/AC, and PDHA/AC electrodes between −0.2 and 1.2 V in 1*M* $LiClO_4$/ACN at a scan rate of 4 mVs^{-1}. The area encircled by CV curve for composite electrodes is obviously larger than that of the AC electrode at the identical sweep rate, due to the existence of oxidation and reduction couple, which can be ascribed to the reaction of quinone in PDMA/AC electrode and hydroquinone/quinone couple in PDHA/AC electrode with the doping and dedoping of Li^+ in the composite. It also shows that the PDHA/AC composite electrode appeared a new redox couple O/R compared with PDMA/AC electrode, which are mainly ascribed to the interaction of quinone and hydroquinone. Among the three CV, the area of the PDHA/AC curve is largest, which indicates that the PDHA/AC electrode has a higher specific capacitance. However, an accurate capacitance value should be obtained from the galvanostatic charge/discharge experiments.

Figure 8(2) exhibits the CV curves of PDHA/AC electrodes measured at various scan rates of 1, 2, and 4 mVs^{-1}, respectively. The current clearly increases with increasing scan rate, showing a good rate capability. Currents rapidly reach a steady state value when the sweep direction changes, and the potential of redox peaks do not shift with the scan rate increase, indicating that the PDHA/AC electrode has stable electrochemical properties.

Glvanostatic Charge/Discharge Analysis. Figure 9(1) shows galvanostatic charge/discharge curves of all electrodes measured at a current density of 0.37 A g^{-1} under a potential window of 0–1.5 V (vs. Ag/AgCl) in 1.0*M* $LiClO_4$/ACN electrolyte. In organic electrolyte, the AC electrode performs an ideal double-layer capacitor behavior with a typical triangular-shaped curve. The curve of the PDMA/AC electrode shows a longer charge/discharge duration owing to the combination of electric double-layer capacitance and faradaic capacitance. The charge/discharge curve of PDHA/AC electrode deviates from the ideal triangular shape: charge/discharge voltage plateau display at 0.3 V and 0.9–1.0 V, as being consistence with the peaks in the CV record

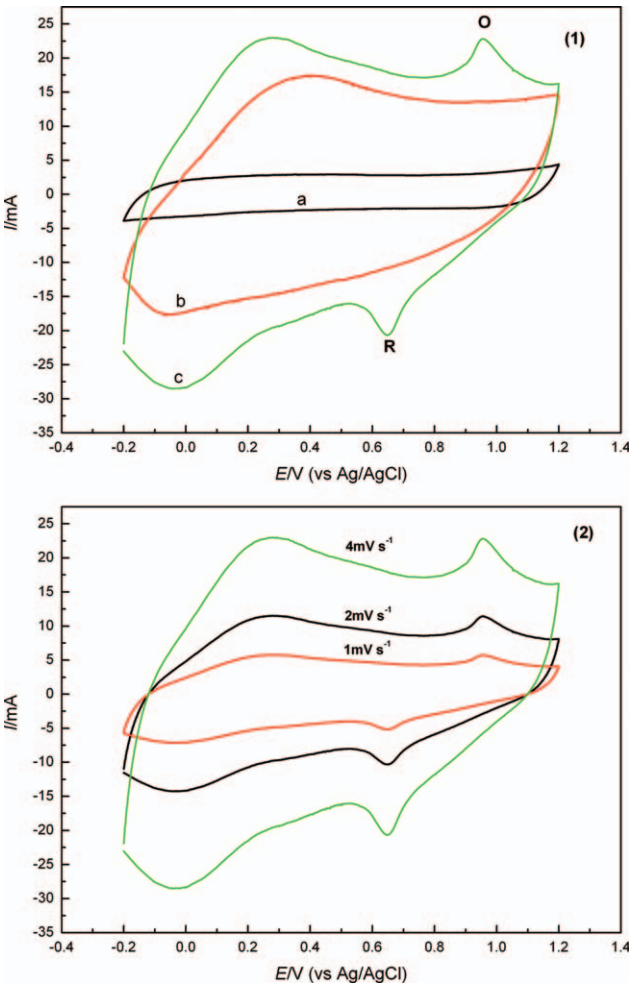

Figure 8. Cyclic voltammograms recorded of the resulting electrodes between −0.2 and 1.2 V (vs. Ag/AgCl) in 1.0*M* $LiClO_4$/ACN: (1) a: AC, b: PDMA/AC, and c: PDHA/AC electrodes at a scan rate of 4 mVs^{-1} and (2) PDHA/AC electrode at different scan rates of 1, 2, and 4 mVs^{-1}. [Color figure can be viewed in the online issue, which is available at wileyonlinelibrary.com.]

Applied Polymer SCIENCE

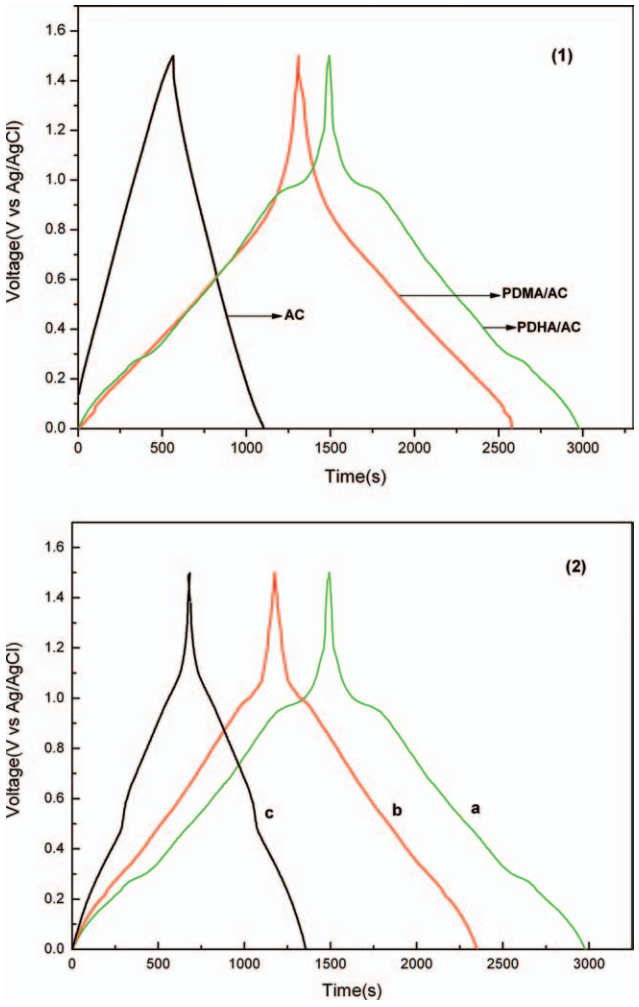

Figure 9. Galvanostatic charge/discharge tests under a potential window of 0–1.5 V (vs. Ag/AgCl) in 1.0*M* $LiClO_4$/ACN: (1) AC, PDMA/AC, and PDHA/AC electrodes at a current density of 0.37 A g^{-1} and (2) PDHA/AC electrode at different current density: (a) 0.37 A g^{-1}, (b) 0.56 A g^{-1}, and (c) 0.93 A g^{-1}. [Color figure can be viewed in the online issue, which is available at wileyonlinelibrary.com.]

reflected in Figure 8, reflecting the process of a faradic reaction caused by the existence of hydroquinone/quinone couple in the PDHA composite. The average discharge SC of these electrodes can be calculated on the basis of the following equation[36]:

$$Cm = \frac{I \times \Delta t}{\Delta V \times m} \tag{2}$$

Because the discharge curve of the composite electrodes is not ideal straight line, so discharge potential is calculated by integral as followed:

$$\Delta V = \frac{\int V dt}{\Delta t} \tag{3}$$

where C_m is the specific capacitance, I is the constant discharge current, t is the discharge time, ΔV is the average discharge potential, and m is the mass of active material within the electrode.

Table I. Specific Capacitance of AC and Composite Electrodes at a Current Density of 0.37 A g^{-1} Under a Potential Window of 0–1.5 V (vs. Ag/AgCl) in 1.0*M* $LiClO_4$/ACN

Electrode	AC	PDMA/AC	PDHA/AC
Specific capacitance (F g^{-1})	127	751	975
Mass (mg)	3.8	6.2	5.4

The SCs of these electrodes obtained from Figure 9(1) are listed in Table I. In the organic electrolyte, the SC of the PDHA/AC composite electrode is 975 F g^{-1}, which is much higher than that of PDMA/AC composite electrode (751 F g^{-1}) at a current density of 0.37 A g^{-1} between 0.0 and 1.5 V due to the existence of the introduced hydroquinone. Therefore, further electrochemical investigations are focused on the PDHA/AC composite in this study as follows.

Figure 9(2) shows the galvanostatic charge/discharge curve of PDHA/AC electrodes measured at various current densities of 0.37, 0.56, and 0.93 A g^{-1}. All the charge curves are very symmetric to their corresponding discharge counterparts, which means that a reversible redox occurs among the electrode materials. The SCs of PDHA/AC composite electrodes at different current densities of Figure 9(2) are listed in Table II. The SC decreases slightly with the increase of charged/discharge current density which reveals good rate ability of the PDHA/AC electrode, it is very important for the electrode materials of a supercapacitor to provide high-power density.

Cycle Life Test. Since degradation of conducting polymers is usually found during the charge/discharge cycles,[37] cycle life is very important to the electrode material, so the stability of the electrode has to be examined in order to evaluate its practical applicability. Typical galvanostatic charge/discharge cycling results of AC electrode, PDHA/AC electrode and PDHA film deposited on glassy carbon electrode at current densities of 0.93 A g^{-1} in the potential range of 0.0–1.5 V for 500 cycles are employed to investigate the cyclic life. Figure 10 shows the discharge specific capacitance of these electrodes as a function of cycle numbers. During the initial cycle, capacitance of 940 F g^{-1} is obtained of PDHA/AC electrode, this value reduced to 810 F g^{-1} after 500 cycles. The capacitance retention of PDHA/AC composite electrode is about 86.2%, the capacitance retention of AC electrode is about 91%, and the capacitance retention of PDHA film is about 63% during the charge/discharge cycles. The capacitance decay is probably due to the degradation of PDHA during cycling. Swelling and deswelling of this

Table II. Specific Capacitance of PDHA/AC Composite Electrode at Various Current Densities of 0.37, 0.56, and 0.93 A g^{-1} Under a Potential Window of 0–1.5 V (vs. Ag/AgCl) in 1.0*M* $LiClO_4$/ACN

Current density (A g^{-1})	0.37	0.56	0.93
C_m (F g^{-1})	975	957	940

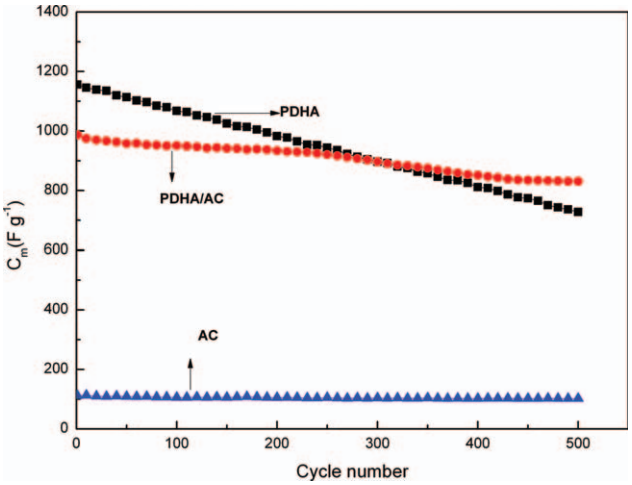

Figure 10. The cycle life test of different electrodes at a current densities of 0.95 A g^{-1} in the potential range of 0.0–1.5 V for 500 cycles (vs. Ag/AgCl) in 1.0*M* $LiClO_4$/ACN. [Color figure can be viewed in the online issue, which is available at wileyonlinelibrary.com.]

electroactive polymer may also lead to degradation. PDHA/AC electrode combines with the advantage of the stability of AC and the high capacity performance of PDHA.

Electrochemical Impedance Spectroscopy Analysis. From the redox peaks voltage of CV test and voltage plateaus of galvanostatic charge/discharge curves, it can be inferred that the conductance of PDHA is maximum at ~ 1.0 V. Therefore, typical Nyquist diagrams for the AC, PDHA, and PDHA/AC electrodes in 1*M* $LiClO_4$/ACN measured at applied potential of 1.0 V are shown in Figure 11.

The impedance spectra are almost similar in shape, composed of a single semicircle in the middle frequency region and a sloped line in the low frequency region. The resistance value of the high frequency intercept of the semicircle with the real axis is represented for the bulk resistance (R_s), which included the ionic resistance of electrolyte, the intrinsic resistance of the active material, and the contact resistance at the interface active material/current collector.[38]

From Figure 11, it can be obviously found that the R_s of PDHA is smallest than that of PDHA/AC and AC. Since the electrolyte and current collector of all capacitor systems are identical, it is indicated that the conductance of PDHA is larger than that of AC.

A semicircular was observed in the middle frequency region, revealing charge-transfer resistance.[39] Charge-transfer resistance reflects the impedance of the activation process of faraday impedance. The charge-transfer resistance of composite electrode is mainly caused by the interactions of the electrolyte and PDHA film on the surface of the electrode. From the redox peaks voltage of CV test, it can be inferred that PDHA is in emeraldine(E)[22] state at ~ 1.0 V, at this state PDHA has pseudofaradaic reactions, and the conductance of PDHA/AC electrode is much higher than that of AC electrode (the R_s of PDHA/AC is smaller than that of AC). It is clearly seen that PDHA/AC electrode includes a semicircle with smaller diameter than AC electrode, which indicates the charge-transfer resistance of PDHA/AC is lower than AC electrode.

In the low frequency the impedance plot exhibited a slightly tilted vertical line characteristic of a limiting diffusion process, which is characteristic feature of capacitive behavior.[40,41] For the line in the low frequency, the more tendency to vertical represent the better performance of capacitance behavior. It is clearly seen that PDHA shows a best capacitance behavior, due to PDHA's pseudofaradaic reactions at this potential and the porous morphology. It also shows that PDHA/AC electrode displays a better capacitance behavior than AC electrode.

At applied potential of 1.0 V, resistance of the PDHA/AC composite is lower than that of AC, it is further proved that PDHA/AC electrode may have excellent active sites and conductivity, which provides high SC and facilitates the charge transfer process. The result also demonstrates that PDHA/AC composite has high-power characteristics and is a kind of very promising material for application of supercapacitors in organic electrolyte.

Supercapacitive Properties of PDHA/AC Composite Electrode. In order to further investigate the supercapacitive performance of PDHA/AC composite electrode under a higher potential, an asymmetric capacitor, respectively using PDHA/AC composite electrode and AC electrode as the positive and negative electrode materials was assembled. For comparison purpose, a symmetric capacitor containing two identical pure AC electrodes was also fabricated. Figure 12 shows the third charge/discharge curves of the capacitor cells. The charge/discharge cycle for the cell was performed in 1*M* $LiClO_4$/ACN at a constant current of 0.93 A g^{-1} between 0 and 2.0 V.

The discharge curve of the asymmetric and symmetric capacitor show a typical capacitive behavior with a linear slope. The specific ED and power density (PD) were calculated by following equations from the constant current charge/discharge cycle:

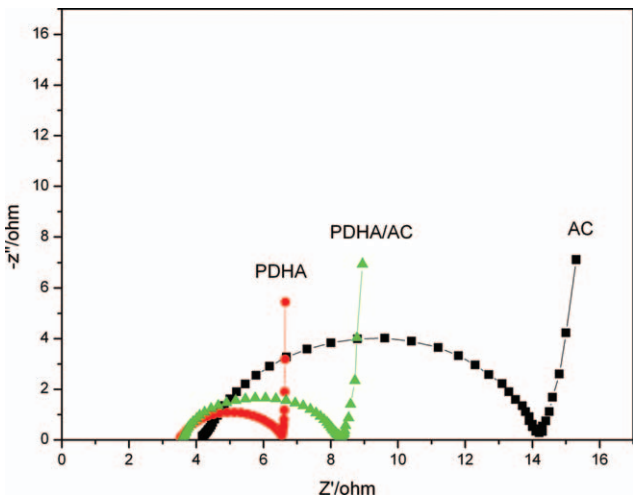

Figure 11. Electrochemical impedance plots of different electrodes (vs. Ag/AgCl) in 1.0*M* $LiClO_4$/ACN. [Color figure can be viewed in the online issue, which is available at wileyonlinelibrary.com.]

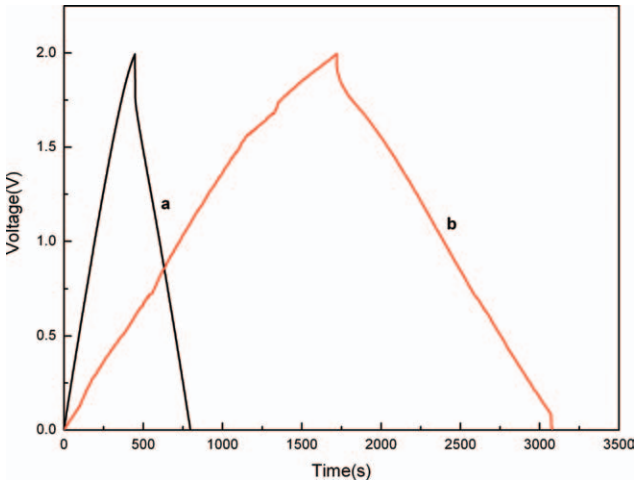

Figure 12. Third charge/discharge curves of the supercapacitor at a current densities of 0.95 A g^{-1} in the potential ranges of 0.0–2.0 V. (a) Symmetric capacitor containing two identical pure AC electrodes and (b) asymmetric capacitor using PDHA/AC and AC as the positive and negative electrode. [Color figure can be viewed in the online issue, which is available at wileyonlinelibrary.com.]

$$\mathrm{ED} = \frac{1}{2}\mathrm{CV}^2 \ \left(\mathrm{Wh\ kg^{-1}}\right) \tag{4}$$

$$\mathrm{PD} = \frac{E}{t} \ \left(\mathrm{W\ kg^{-1}}\right) \tag{5}$$

where C is the specific capacitance of the capacitor, V is the potential range from the end of the charge to the end of the discharge, and t is the discharge time.

Using these equations, the ED of the asymmetric capacitor is 178 $\mathrm{Whkg^{-1}}$ at a power density of 474 W $\mathrm{kg^{-1}}$ based on the total weight of AC and PDHA/AC composite electrodes, while the symmetric capacitor shows a ED of 39 $\mathrm{Whkg^{-1}}$ and a power density of 350 W $\mathrm{kg^{-1}}$ according to the weight of active material in both electrodes. The power density and ED of asymmetric capacitor is higher than those of the symmetric capacitor, which can be explained on basis of the faradic reaction in composite electrode. This result reveals the asymmetric capacitor containing PDHA/AC electrode show a great capacitor performance using organic electrolyte.

CONCLUSIONS

PDHA film was successfully prepared by electrochemical method on the surface of AC electrodes. FTIR spectroscopy and CV measurements indicated the presence of hydroquinone units in PDHA. At a current density of 0.93 A g^{-1}, the SC of PDHA/AC electrode was 940 F g^{-1} and the composite electrode showed a capacity fade of only 13.8% after 500 cycles. The ED of asymmetric capacitor which consists of PDHA/AC positive and AC negative electrodes was 178 $\mathrm{Whkg^{-1}}$ at a power density of 474 W $\mathrm{kg^{-1}}$. This result reveals the asymmetric capacitor containing PDHA/AC electrode shows a great capacitor performance using organic electrolyte.

ACKNOWLEDGMENTS

This work was supported by National Natural Science Foundation of China (50903078), Specialized Research Fund for the Doctoral Program of Higher Education (New Teachers) (20090132120017), Promotive Research Fund for Excellent Young and Middle-Aged Scientists of Shandong Province (BS2009CL036), the Natural Science Foundation of Shandong Province of China (ZR2011BQ017), and the Fundamental Research Funds for the Central Universities (201013045).

REFERENCES

1. Rudge, A.; Raistrick, I.; Gottesfeld, S.; Ferraris, J. P. *Electrochim. Acta.* **1994,** *39*, 273.
2. Ryu, K. S.; Kim, K. M.; Park, N. G.; Park, Y. J.; Chang, S. H. *J. Power Sources.* **2002,** *103*, 305.
3. Rudge, A.; Raistrick, I.; Gottesfeld, S.; Ferraris, J. P. *Electrochim. Acta.* **1994,** *39*, 273.
4. Koysuren, O.; Du, C. S.; Pan, N.; Bayram, G. J. *Appl. Polym. Sci.* **2009,** *113*, 1070.
5. Su, C.; Wang, G. C.; Huang, F. J. *Appl. Polym. Sci.* **2007,** *106*, 4241.
6. Li, L. M.; Liu, E. H.; Shen, H. J.; Yang, Y. J.; Huang, Z. Z.; Xiang, X. X.; Tian, Y. Y. *J. Solid State Electrochem.* **2011,** *15*, 175.
7. Mu, S.; Chen, C.; Wang, J. *Synth. Met.* **1997,** *88*, 249.
8. Jureviciute, I.; Bruckenstein, S. J. *Solid State Electrochem.* **2003,** *7*, 554.
9. Oztemiz, S.; Beaucage, G.; Ceylan, O. J. *Solid State Electrochem.* **2004,** *8*, 928.
10. Kelly, T. L.; Yano, K.; Wolf, M. O. *ACS Appl. Mater. Interfaces.* **2009,** *1*, 2536.
11. Kazim, S.; Ahmad, S.; Pfleger, J.; Plestil, J.; Joshi, Y. M. *J. Mater. Sci.* **2012,** *47*, 420.
12. Li, D. F.; Wang, H. G.; Wang, X. K. *J. Mater. Sci.* **2007,** *42*, 4642.
13. Deepa, M.; Ahmad, S.; Alam, J.; Ahmad, S.; Sood, K. N.; Srivastava, A. K. *Electrochim. Acta.* **2007,** *52*, 7453.
14. Cai, J. J.; Zuo, P. J.; Cheng, X. Q.; Xu, Y. H.; Yin, G. P. *Electrochem. Commun.* **2010,** *12*, 1572.
15. Shi, S.; Zhang, L.; Li, J. J. *Mater. Sci.* **2009,** *44*, 945.
16. Hosseini, M. G.; Sabouri, M.; Shahrabi, T. *Prog. Org. Coat.* **2007,** *60*, 178.
17. Tamai, H.; Hakoda, M.; Shiono, T.; Yasuda, H. J. *Mater. Sci.* **2007,** *42*, 1293.
18. Abdiryim, T.; Jamal, R.; Nurulla, I. J. *Appl. Polym. Sci.* **2007,** *105*, 576.
19. Shi, J.; Wang, Z.; Li, H. L. *J. Mater. Sci.* **2007,** *42*, 539.
20. Patil, V.; Sainkar, S. R.; Patil, P. P. *Synth. Met.* **2004,** *140*, 57.
21. D'Aprano, G.; Leclerc, M.; Zotti, G. J. *Electroanal. Chem.* **1993,** *351*, 145.
22. Huang, L. M.; Wen, T. C.; Gopalan, A. *Synth. Met.* **2002,** *130*, 155.

23. Palys, B.; Kudelski, A.; Stankiewicz, A.; Jackowska, K. *Synth. Met.* **2000,** *108*, 111.
24. Liu, L.; Wang, W.; Zou, W. Y. *J. Solid State Electrochem.* **2010,** *14*, 2219.
25. Nam, K. W.; Lee, C. W.; Yang, X. Q.; Cho, B. W.; Yoon, W. S.; Kim, K. B. *J. Power Sources.* **2009,** *188*, 323.
26. Fischer, A. E.; Pettigrew, K. A.; Rollison, D. R.; Stroud, R. M.; Long, J. W. *Nano. Lett.* **2007,** *7*, 281.
27. Wan, C.; Azumi, K.; Konno, H. *Electrochim. Acta.* **2007,** *52*, 3061.
28. Zhu, S.; Zhou, H.; Hibino, M.; Honma, I.; Ichihara, M. *Adv. Funct. Mater.* **2005,** *15*, 381.
29. Dong, X.; Shen, W.; Gu, J.; Xiong, L.; Zhu, Y.; Li, H.; Shi, J. J. *Phys. Chem. B.* **2006,** *110*, 6015.
30. Zou, W. Y.; Wang, W.; He, B. L.; Sun, M. L.; Yin, Y. S. *J. Power Sources.* **2010,** *195*, 7489.
31. Patil, V.; Sainkar, S. R.; Patil, P. P. *Synth. Met.* **2004,** *140*, 57.
32. Socrates, G. Infrared Characteristic Group Frequencies, 2nd ed.; Wiley: New York, **1994.**
33. Sariciftci, N. S.; Kuzmany, H. *Synth. Met.* **1987,** *21*, 157.
34. Anwar-ul-Haq, A. S. Electrochemical Synthesis and Spectroelectrochemical Characterization of Conducting Copolymers of Aniline and o-Aminophenol. Ph.D. Thesis, Institute of Chemistry, Chemnitz University of Technology, Germany. January 2007.
35. Malinauskas, A. *Synth. Met.* **1999,** *107*, 75.
36. Dong, B.; He, B. L.; Xu, C. L.; Li, H. L. *Mater. Sci. Eng. B.* **2007,** *143*, 7.
37. He, B. L.; Dong, B.; Wang, W.; Li, H. L. *Mater. Chem. Phys.* **2009,** *114*, 371.
38. Nian, Y. R.; Teng, H. J. *Electrochem. Soc.* **2002,** *149*, A1008.
39. Guo, D. J.; Li, H. L. *J. Solid State Electrochem.* **2005,** *9*, 445.
40. Mi, H. Y.; Zhang, X. G.; Yang, S. D.; Ye, X. G.; Luo, J. M. *Mater. Chem. Phys.* **2008,** *112*, 127.
41. Gabrielli, C.; Keddam, M.; Nadi, N.; Perrot, H. J. *Electroanal. Chem.* **2000,** *485*, 101.